

VVRRM: Vehicular Vibration-based Heart RR-Interval Monitoring System

Amelie Bonde
Carnegie Mellon University
Electrical and Computer Engineering
Moffett Field, California
amelie@cmu.edu

Shijia Pan
Carnegie Mellon University
Electrical and Computer Engineering
Moffett Field, California
shijiapan@cmu.edu

Zhenhua Jia
Rutgers University
Wireless Information Network
Laboratory
North Brunswick, New Jersey
zhenhua@winlab.rutgers.edu

Yanyong Zhang
Rutgers University
Wireless Information Network
Laboratory
North Brunswick, New Jersey
yyzhang@winlab.rutgers.edu

Hae Young Noh
Carnegie Mellon University
Civil and Environmental Engineering
Pittsburgh, Pennsylvania
noh@cmu.edu

Pei Zhang
Carnegie Mellon University
Electrical and Computer Engineering
Moffett Field, California
peizhang@cmu.edu

ABSTRACT

Continuous heart rate variability (HRV) monitoring in cars can allow ambient health monitoring and help track driver stress and fatigue. Current approaches that involve wearable or externally mounted sensors are accurate but inconvenient for the user. In particular, prior approaches often fail when noise from human motion or car noise are present.

In this paper, we present *VVRRM*, an ambient heartbeat monitoring system in an automobile which uses a set of accelerometers in a car seat to monitor a subject's heart RR-intervals. The system removes high energy motion noise and periodic noise using a combination of peak detection with extracted wavelet coefficients. Furthermore, it tracks human heart locations through sensor selection to maximize the heart signal energy. We tested the system with both a manufactured heartbeat signal and experiments with human subjects. Overall our mean absolute error for RR-interval estimation was 54 ms across all human subjects, and 3 ms with our manufactured heartbeat signal.

CCS CONCEPTS

• **Human-centered computing** → **Ubiquitous and mobile computing systems and tools**;

KEYWORDS

vibration; heart rate variability (HRV); vehicular sensing; human condition monitoring

ACM Reference Format:

Amelie Bonde, Shijia Pan, Zhenhua Jia, Yanyong Zhang, Hae Young Noh, and Pei Zhang. 2018. *VVRRM: Vehicular Vibration-based Heart RR-Interval Monitoring System*. In *Proceedings of 19th International Workshop on Mobile Computing Systems & Applications (HotMobile '18)*. ACM, New York, NY, USA, 6 pages. <https://doi.org/10.1145/3177102.3177110>

1 INTRODUCTION

Continuous heart rate and heart rate variability (HRV) monitoring in cars can allow for ambient health monitoring in an environment people inhabit regularly. Short-term heart rate variability monitoring in terms of RR-intervals (the distance between successive heartbeats) is particularly useful. It has been used to help track stress and fatigue, which are important driver safety issues [4, 13, 16].

Prior work takes a number of approaches including photoplethysmography, electrocardiography (ECG) and cameras, sometimes in combination, to retrieve heart rate from people [8, 9, 14, 18]. These methods can be useful for heart-rate monitoring in static environments but are inconvenient to the user or are inaccurate for RR-interval measurements. In particular, these approaches fail for high-noise in-car environments subject to periodic noise such as car engine vibration and impulsive noise from subject movement.

We present *VVRRM*, a non-intrusive, heart RR-interval measurement system for the in-car environment. *VVRRM* first collects accelerometer data from our sensing module embedded in car seats. We then remove high-energy non-periodic motion segments resulting from body motion and periodic noise resulting from the engine and other noise. We choose between multiple sensors to account for variations in body size and position. Finally, we perform peak detection to obtain the RR-interval using the distance between the peaks.

We chose to study an idling car instead of a driving scenario because we wanted to focus on engine and human motion noise before tackling the noise caused by the car's movement on the road. We felt the noise of the moving car would overwhelm the other types of noise and should be studied separately.

Our paper provides three contributions:

Permission to make digital or hard copies of all or part of this work for personal or classroom use is granted without fee provided that copies are not made or distributed for profit or commercial advantage and that copies bear this notice and the full citation on the first page. Copyrights for components of this work owned by others than ACM must be honored. Abstracting with credit is permitted. To copy otherwise, or republish, to post on servers or to redistribute to lists, requires prior specific permission and/or a fee. Request permissions from permissions@acm.org.

HotMobile '18, February 12–13, 2018, Tempe, AZ, USA

© 2018 Association for Computing Machinery.

ACM ISBN 978-1-4503-5630-5/18/02...\$15.00

<https://doi.org/10.1145/3177102.3177110>

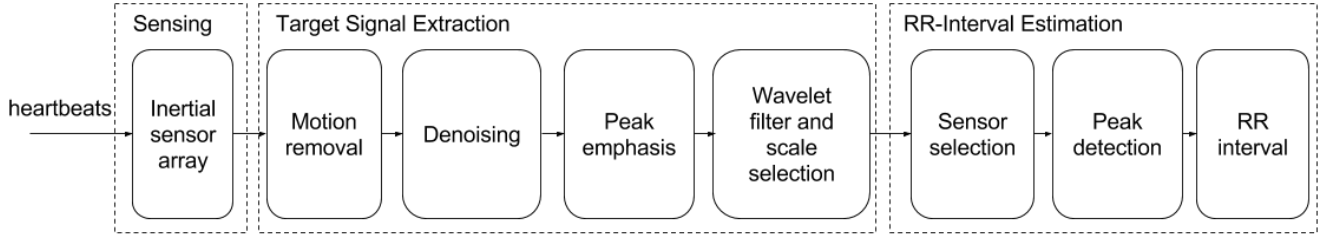


Figure 1: System Overview

- (1) We introduce *VVRRM*, a real-time system that uses ambient car seat vibration to monitor the RR-intervals of a subject in a (currently stationary) car.
- (2) We characterize the motion noise caused by human movement and the motion noise caused by an idling car and present an adaptive sensing algorithm to detect the heartbeat signal in the midst of high levels of noise.
- (3) We present a comprehensive evaluation of our system using both characterization data with heartbeat recordings and human subject experiments.

The rest of this paper is organized as follows: We discuss related work in Section 2, and also discuss background information related to heart rate and heart rate variability. Section 3 describes our overall system, and we describe our evaluation and go over results in Section 4. Finally, in Section 5 we conclude our work.

2 BACKGROUND AND RELATED WORK

Definition of Heart RR-Interval: At every beat, the heart is polarized and depolarized to trigger its contraction, an electrical activity which can be measured by an ECG. The depolarization of the main mass of the ventricle causes the largest peak in an ECG, called the R wave. The RR-interval is defined as the distance between the peaks of two R waves and describes the duration of one complete cardiac cycle. The peaks of the waves *VVRRM* measures correspond to the heart’s movement, and the distance between the two peaks is the same as the RR-interval.

Heart RR-interval as an Indicator of Stress: As stress level increases, the heart rhythm is affected and becomes unstable [3]. This instability is reflected in RR-interval measurements [11]. Thus RR-intervals provide a key indicator of stress. Prior work in the medical domain has defined that the error of this indicator needs to be lower than 100ms [6].

Monitoring Methods: Various ways of monitoring heart rate have been explored in the noisy vehicle environment. One common approach relies on the use of electrocardiogram (ECG) sensors [5, 9, 17]. These approaches, in general, require mounting that allows direct skin contact between the driver and the sensors to avoid unacceptable noise levels. While their performance is promising, this mounting requirement prevents these approaches from becoming mainstream.

Wearable devices can be inconvenient for the user, so we prefer an approach that is integrated with the car. A variety of approaches have been tried including the use of capacitive sensors in the seat, high-resolution cameras to capture skin tone fluctuations,

and thermal imaging. While these approaches work well in a static environment in the lab, in the vehicle they are subject to non-ideal situations (e.g. light conditions, vibrations, etc.), these approaches fail to provide accurate measurements of individual heartbeat intervals [2, 14, 18], which is not useful for stress and fatigue inference. Placing sensors in a steering wheel is also subject to real-world problems, as drivers place their hands in different positions and often wear gloves in cold weather[8].

In non-vehicle environments, vibration-based approaches have been utilized in beds [7]. These approaches utilize the mechanical motion of the heart to detect and sense heartbeat without intrusive sensors. These approaches hold promise for non-skin-contact sensing. Unlike vibration-based approaches, capacitive sensors that are not worn next to the body can be sensitive to environmental noise, including noise that does not involve motion (e.g., humidity, the distance of body parts from the sensor), while accelerometers only measure motion from the parts of the body they are in contact with. (e.g., if a person moves a part of the body not in contact with the accelerometer, such as their arms, the sensor values do not change significantly due to motion). This means that when using accelerometers, the noise sources would be greatly reduced. Using accelerometers has some limitations: along with motion noise and placement concerns, which we address, they may be sensitive to clothing thickness.

3 SYSTEM DESCRIPTION

VVRRM accurately detects the vibration of heartbeats through the body’s forces on the car seat in an automobile to measure RR-intervals. This poses many challenges which our system addresses with a multifold approach. Our main challenges are the sometimes low signal to noise ratio (heartbeat forces on the seats are small), human motion noise (movement noise can overwhelm the signal), engine noise (periodic engine noise increases the noise floor), and sensor placement (the best location to capture the heart motion varies between persons and over time. We can intuitively understand this because people are different heights and they sit in different ways). Figure 1 shows the system overview. The sensing module acquires the signal using a grid of accelerometers to capture the heart motion that can occur at **different locations**. The target signal extraction module removes high motion parts induced by **human motion**. Then it performs denoising on the remaining signal to remove **periodic noise** (e.g. engine noise). Next, it smooths the signal to **enhance peaks**, followed by a wavelet filter to further enhance the impulse signal in the heart rate frequency range.

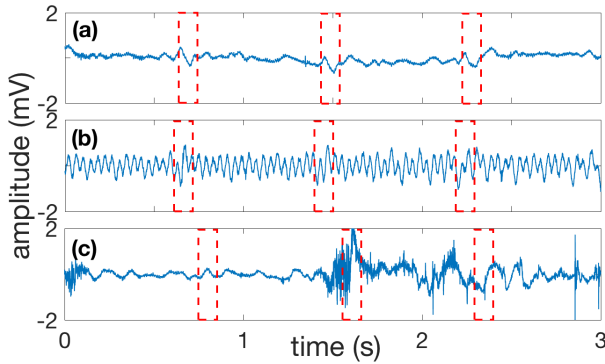


Figure 2: Raw data for a human subject with (a): engine off, (b): engine on, and (c) with subject laughing. Red boxes mark the heartbeat location. With no engine noise, the heartbeat signal in (a) is fairly clear. In (b), it is harder to see because of engine noise, while in (c), it is obscured by noise from laughter.

Finally, the RR-interval estimation module addresses the sensor placement challenge with a sensor selection algorithm, and outputs the final RR-interval estimation.

3.1 Sensing

VVRRM uses a set of inertial sensors to pick up movement caused by the subject’s beating heart as the subject sits in the seat. The heartbeat causes their chest and stomach to vibrate. Because we detect the vibration of heartbeats from the vibration of the seat, the location of the sensor relative to the body greatly impacts the signal magnitude. Intuitively, the closer the sensor is to the heart, the stronger the signal. This raises two challenges: 1) People are different heights, so when they sit in the car their hearts are in different locations. And 2) people sometimes shift position and do not always sit leaning back. To address the first challenge, we use a network of sensors that lie against the backrest of the car seat and can pick up signals from a larger area. To address the second challenge, we use a sensor in the seat belt to pick up the stomach vibration caused by the heartbeat. We choose a sparse sensor array instead of many sensors for a lower-cost and low-computational-power design. We use piezoelectric accelerometers, which are excellent for vibration monitoring due to their wide frequency response, linear frequency response curve, and high sensitivity. We describe the sensor selection algorithm in Section 3.3.1.

Accelerometers are very sensitive to vibration and changes in motion: this allows us to see the very small signal caused by the motion of the beating heart. Figure 2(a) shows raw data from a human subject sitting in a car. We can see clear heartbeat-induced vibrations as small peaks marked by the dashed red boxes. That same sensitivity also makes accelerometers very sensitive to vibration and motion noise. Figure 2(b) shows a human subject sitting in an idling car. The **engine noise** makes the heartbeat signal less clear. Figure 2(c) shows a human subject laughing. The **human motion noise** of laughter completely overwhelms the heartbeat signal. We describe how VVRRM handles these types of noise in the following sections.

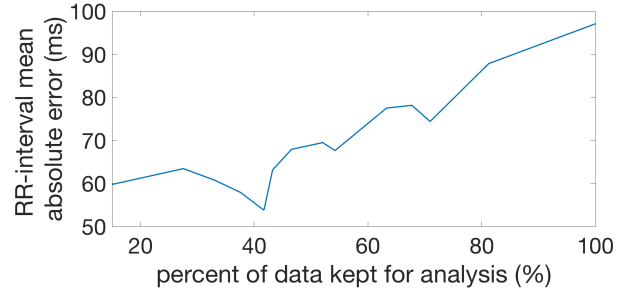


Figure 3: As we lower our noise threshold and keep less data, our error lowers and then increases.

3.2 Target Signal Extraction

The target signal extraction module handles both human motion and engine noise. It first extracts windows of data where there is less human motion noise. It then applies denoising and a wavelet filter to remove engine noise.

3.2.1 Windowing for Human Motion Noise Extraction. Our first step is recognizing and discarding portions of the signal that are excessively noisy due to person movement. We found that most large spikes of noise in the data were due to person movement, either talking, coughing, laughing, gesturing, or shifting positions. To identify this type of signal, we use a sliding window on the vibration signal and extract the maximum value of the window. If this value is above a threshold, we skip one second of data (i.e., label it as motion noise) and try again with a new window, moving forward by one second each time until we have a window that doesn’t exceed our threshold. We skip one second at a time because we observe experimentally that noise in the data tends to last from between half a second to several seconds and takes about half a second to subside. We set our threshold by fitting a probability distribution to the first minute of data for each person using kernel density estimation and then using the inverse cumulative distribution function (ICDF) to compute a threshold to detect high motion noise. The threshold is determined empirically, considering the tradeoff between data preservation and accuracy (i.e., high threshold leads to more data but lower accuracy, while low threshold increases accuracy but wastes lots of data).

We note that as we lower our noise threshold, there are sometimes small peaks that buck the general trend. This is because our thresholding method occasionally cuts out some data that gives good results, causing a small rise in our error. We observe that at about 41% of data from the optimal sensor kept across all subjects, the error starts to rise. Setting the threshold to the ICDF function for 89% minimizes this error.

3.2.2 Denoising for Engine Noise Reduction. We then do denoising to further reduce the noise in the signal. We place one sensor near the bottom of the backrest, away from the heart, to characterize noise. We observed that the level of noise recorded by each sensor is different, so it works best to partially subtract one sensor’s signal from the other. We multiply the noise sensor signal by a fraction (we obtained 20% heuristically) and subtract it from the rest of the sensors.

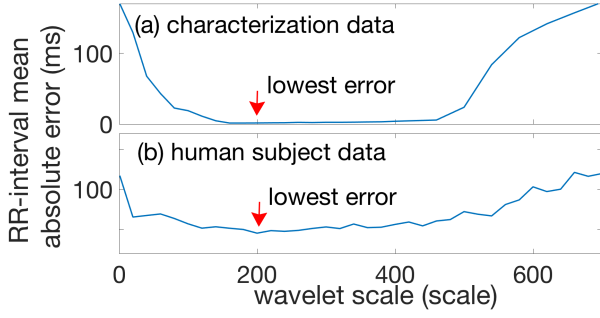


Figure 4: The mean absolute RR-interval error with different wavelet scales, (a), with characterization data, and (b) with human subject data. Using a scale of 200 minimized our error.

3.2.3 Peak Emphasis to Enhance Heartbeat Signal. In order to enhance the weak peaks of the heartbeat signal, we do root-mean-square averaging, which preserves the peaks in the data and smooths the high-frequency noise.

3.2.4 The Continuous Wavelet Transform for Heartbeat Isolation. To further reduce the noise, we isolate the periodic nature of the heartbeat using a continuous wavelet transform (CWT)[1]. The CWT compares the signal to compressed and stretched versions of a wavelet, the CWT's analyzing function. The Mexican hat wavelet has been widely used for characterizing impulse signals, which fits our target signal profiling. It is described by

$$\psi(t) = \frac{2}{\sqrt{3}\pi^{\frac{1}{4}}}(1-t^2)e^{-\frac{t^2}{2}} \quad (1)$$

The stretching and compressing of the wavelet performed by the CWT is known as "scaling": the CWT is a function of scale (a) and position (b):

$$C(a, b; f(t), \psi(t)) = \int_{-\infty}^{\infty} f(t) \frac{1}{a} \psi\left(\frac{t-b}{a}\right) dt \quad (2)$$

$f(t)$ is the signal, t is time, and $\psi(t)$ is the wavelet function.

By varying the values of the scale parameter, a , and the position parameter, b , we obtain the cwt coefficients $C(a, b)$. We chose the scale that best represents our data and varied the position coefficients to obtain a one-dimensional filtered signal. Figure 4 shows the result of the wavelet transform using scales between 1 and 700. *VVRRM* chose the scale that gives the lowest error, in this case, scale 200. Scale 200 corresponds to a frequency of 2.5 Hz, which, at 150 beats per minute, is higher than any heart rate we expect to see. This makes sense because the heartbeat is made up of several components, described in the background section. Choosing too low a frequency would lose information from these different components, while too high a frequency wouldn't filter out engine noise.

3.3 RR-Interval Estimation

Once the signal is enhanced and filtered, we calculate RR-interval with the sensor with the highest signal amplitude.

3.3.1 Sensor Selection. To adapt to a wide range of heart positions with sparse sensors, we displace the sensors with minimum overlapping sensing range and choose the sensor closest to the heart. In each window, we calculate the mean of the wavelet coefficients for each sensor, and select the one with highest mean, indicating highest Signal-to-Noise Ratio. This algorithm depends on our having removed noisy parts in the signal and reduced the noise in the remaining signal, as high amounts of noise could also cause a higher mean, and cause the incorrect selection of a sensor as "optimal".

3.3.2 Peak Detection for Peaks of Heartbeat Motion. For the first step in our peak detection algorithm, we do root-mean-square averaging of the wavelet coefficients, which smooths the data, limiting small false peaks and emphasizing larger peaks. We find local maxima by calculating the derivative of our signal in two points in time and comparing them to see if the difference lies above a given threshold [10]. Then we pick points near the local maxima and apply Least Squares Curve Fitting over them to refine the peak location [10].

3.3.3 RR-Interval Estimation. We occasionally detect extra peaks or drifted peaks from noise in the signal, which we remove to get accurate RR-intervals. Since heartbeats occur at periodic intervals, we discard the lowest magnitude peak of any pair of peaks that are closer than 220 beats per minute, which we take as our maximum heart rate (well above the normal resting heart rate of 60-100 beats per minute). This will not affect HRV monitoring in healthy subjects, because while heart rate does oscillate over time, it is not so irregular that it would have beats this close together and maintain a normal heart rate. Then we find the distance in time between the first two peaks in our sliding window and consider that our RR-interval. Now that we have our RR-interval, we take our next window of data starting at a location just past the 1st peak, ensuring that we don't miss any heartbeats as we move the window forward.

4 EXPERIMENTATION AND CHARACTERIZATION

We evaluated our system with two sets of experiments: controlled heartbeat characterization input, and uncontrolled human subject input.

4.1 Experimental Setup

We use the W354C03_010G10 piezoelectric accelerometer, sampled at 2 kHz [12]. We chose to put the sensors on the passenger seat because passengers move more freely and would give us more varied motion noise. We plan to test the system with steering and other driving motions in a future driving scenario. We put sensors at different heights on the backrest to accommodate different heights of drivers and passengers. The sensor layout is shown in Figure 5. For the characterization experiments, we have three sensors at different heights on the backrest (sensors 1, 2, and 3), while for the human subject experiments we put two sensors on the backrest at different heights and one sensor on the seat belt across the lap (sensors 1, 2, and 5). This is so that if the person leans forward, we can still pick up the motion of the heartbeat through their stomach. Sensor 4, the noise sensor, helps us characterize and remove the

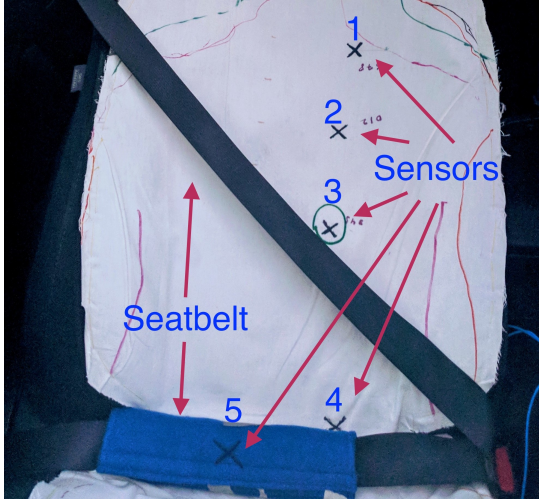


Figure 5: Hardware setup. Sensor 3 was only in characterization experiments, while sensor 5 was only for human subject experiments. Sensor 4 measured noise.

noise in the system. For the characterization experiments, we use a small set of speakers as the input that lean against the seat and play the sound of a heart beating. This allows us to control the height and rate of the heart. For the human subject experiments, we have human subjects sit in the seat, wearing a Zephyr Bioharness belt (capacitive ECG) as the ground truth [15].

4.2 Heartbeat Characterization

In our characterization experiments, we tested different heights and rates of the heart, and different car engine speeds. In order to control heartbeat characteristics in a realistic setting, in our heartbeat characterization experiments, we manufactured a heartbeat signal by putting a set of speakers against the backrest of the car seat, and playing the sound of heartbeats at different rates and with the speakers in different positions against the seat.

To test the effect of heights, we put the simulated heart at 7 different heights against the backrest of the car seat and played heartbeat sounds at 60 BPM. The results are shown in Figure 6(a). Using a single sensor, as the simulated heart got further from the sensor the error increased, but with our sensor selection algorithm, the sensor closest to the heartbeat was consistently chosen and that error was minimized.

4.2.1 Different rates. Figure 6(b) shows the accuracy for different heart rates. In this experiment, we kept the simulated heart in the same place and changed the rate of the heartbeat signal. We found that while there was a small difference in error, with lower heart rates having a slightly larger error, our system performed well across the range. This tells us that our algorithm is not affected by heart rate.

4.2.2 Engine noise evaluation. Figure 6(c) shows the result with the engine revving at different speeds with the car in neutral. We see that different engine speeds did not greatly affect our error. This

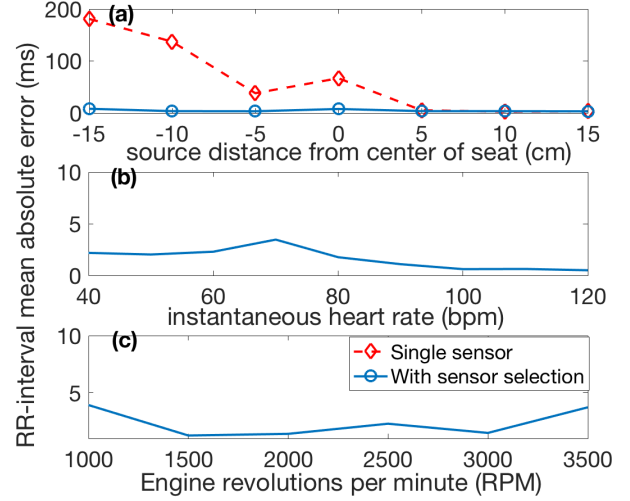


Figure 6: In (a), we compare the sensor selection algorithm with using a single sensor, and see that using sensor selection lowers the average error compared to using a single sensor. In (b), we see that our algorithm is not significantly affected by heart rate. In (c), we see that different engine speeds do not greatly affect error.

shows the continuous wavelet filter effectively removed engine noise.

Overall the mean absolute error for our characterization experiments was 3 ms, and we accurately categorized 100% of our data to within 100 ms of the ground truth (The error of RR-intervals should be lower than 100ms [6]).

4.3 Human Subject Experiments

For our human subject experiments, we asked 4 subjects, 3 men and 1 woman, to sit in an idling car. The participants were between the ages of 25 and 42. We collected 4 minutes of data from each of them for a total of 16 minutes. We noted the time when talking, laughing, coughing, gesturing or shifting positions happened, and found that laughing and coughing caused the most obvious noise in the data. Figure 7 shows the results of the human subject experiments. From this figure, we can see that the system is able to effectively recognize and ignore these noisy parts of the data by fitting a distribution to the data and introducing a threshold, as described in Section 3. When we look at the data by subject, we can see that there is some variation in the data. This can partly be explained by the way the subjects behaved. The extent to which the different subjects talked, laughed, coughed and shifted positions is reflected in the error rate and percent of data under the noise threshold for each subject.

Subject 1 watched funny videos while sitting in the car, and his frequent laughter caused significant noise in the data. However, data with laughing noise was effectively ignored by our algorithm, which greatly reduced both the amount of his data that we used and the error associated with it.

Subject 2 talked frequently and fidgeted. The thresholding algorithm also discarded a lot of her data, but it didn't reduce the

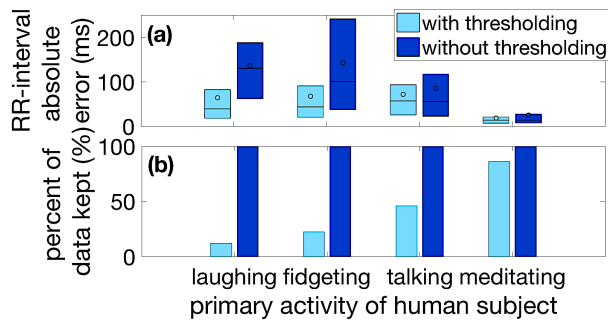


Figure 7: Graph (a) shows the 25% and 75% confidence intervals of the RR-interval absolute error for each human subject. The circles mark the mean error and the horizontal lines mark the median error. (b) shows how much data for each human subject was kept before and after the thresholding algorithm. One can see that there is variation per person in the amount of data under the noise threshold and the error.

error by as much. This could be because some of her periodic fidgeting was confused with heart motion. Subjects 1, 3 and 4 were all between 177 and 180 cm, while subject 2 was 167 cm, significantly shorter than the other subjects. Additionally, the sensor selected for Subject 2 was the one across the lap, while for the other subjects it was a sensor in the backrest. This suggests that either Subject 2 spent a lot of time leaning forward, or the sensors in the backrest were in a bad location to pick up heart rate for shorter subjects. In the future, more subjects with varying heights will help us determine this.

Subject 3 also talked during most of the data collection, with occasional coughing or laughing. This behavior occurred less than subject 1, so less of his data was discarded.

Subject 4 preferred to sit quietly and meditate, so his data had much less motion noise and the lowest error. Subject 4's results suggest that keeping as much data as possible to acquire RR-intervals is a crucial component of obtaining accurate HRV measurements.

Overall the mean absolute error for RR-intervals was 54 ms across all subjects. 84% of our data under threshold was accurately categorized to within the 100 ms error defined in medical literature [6].

5 CONCLUSION

In this paper, we introduced *VVRRM*, a real-time system that uses ambient car seat vibration to monitor the individual heartbeats of a subject in a car. *VVRRM* characterizes and removes the motion noise caused by an idling car and the movement of people, and presents an adaptive sensing algorithm to detect the heartbeat signal in the midst of high levels of noise. Our evaluation shows that we can accurately estimate RR-intervals with the high levels of noise present in an automobile, with on average 54 ms mean absolute error for human subjects and 3 ms mean absolute error for characterization experiments, significantly lower than the 100 ms requirement for RR intervals. Work is still needed to expand

characterization and further noise removal in multiple highway driving scenarios and with more human subjects.

ACKNOWLEDGEMENTS

This research was supported in part by the National Science Foundation (under grants CNS-1149611, CMMI-1653550, CNS-1404118, and CNS-1423020), the National Science Foundation Graduate Research Fellowship Program (under Grant No. DGE 1745016), Intel and Google. The views and conclusions contained here are those of the authors and should not be interpreted as necessarily representing the official policies or endorsements, either express or implied, of Carnegie Mellon University, the National Science Foundation, or the U.S. Government or any of its agencies.

REFERENCES

- [1] MJ Burke and M Nasor. 2012. ECG analysis using the Mexican-Hat wavelet. In *Int. Conf. Multirate Systems & Wavelet Analysis*. 1–6.
- [2] Sergey Y Chekmenov, Aly A Farag, William M Miller, Edward A Essock, and Aruni Bhatnagar. 2009. Multiresolution approach for noncontact measurements of arterial pulse using thermal imaging. In *Augmented vision perception in infrared*. Springer, 87–112.
- [3] Hagit Cohen, Moshe Kotler, Mike A Matar, Zeev Kaplan, Uri Loewenthal, Hanoch Miodownik, and Yair Cassuto. 1998. Analysis of heart rate variability in posttraumatic stress disorder patients in response to a trauma-related reminder. *Biological psychiatry* 44, 10 (1998), 1054–1059.
- [4] Niels Egelund. 1982. Spectral analysis of heart rate variability as an indicator of driver fatigue. *Ergonomics* 25, 7 (1982), 663–672.
- [5] Jennifer A Healey and Rosalind W Picard. 2005. Detecting stress during real-world driving tasks using physiological sensors. *IEEE Transactions on intelligent transportation systems* 6, 2 (2005), 156–166.
- [6] Keri J Heilman, Mika Handelman, Gregory Lewis, and Stephen W Porges. 2008. Accuracy of the StressEraser® in the detection of cardiac rhythms. *Applied psychophysiology and biofeedback* 33, 2 (2008), 83–89.
- [7] Zhenhua Jia, Musaab Alaziz, Xiang Chi, Richard E Howard, Yanyong Zhang, Pei Zhang, Wade Trappe, Anand Sivasubramaniam, and Ning An. 2016. HB-phone: a bed-mounted geophone-based heartbeat monitoring system. In *Information Processing in Sensor Networks (IPSN), 2016 15th ACM/IEEE International Conference on*.
- [8] Boon-Giin Lee and Wan-Young Chung. 2012. A smartphone-based driver safety monitoring system using data fusion. *Sensors* 12, 12 (2012), 17536–17552.
- [9] Nermine Munla, Mohamad Khalil, Ahmad Shahin, and Azzam Mourad. 2015. Driver stress level detection using HRV analysis. In *Advances in Biomedical Engineering (ICABME), 2015 International Conference on*. IEEE, 61–64.
- [10] Thomas C. O'Haver. 2008. Peak finding and measurement. (2008). <https://terpconnect.umd.edu/~toh/spectrum/PeakFindingandMeasurement.htm>
- [11] Massimo Pagani, Raffaello Furlan, Paolo Pizzinelli, Wilma Crivellaro, Sergio Cerutti, and Alberto Malliani. 1989. Spectral analysis of RR and arterial pressure variabilities to assess sympatho-vagal interaction during mental stress in humans. *Journal of hypertension. Supplement: official journal of the International Society of Hypertension* 7, 6 (1989), S14–5.
- [12] PCB Piezotronics. [n. d.]. W354C03_010G10 datasheet. ([n. d.]). http://www.pcb.com/Products.aspx?m=W354C03_010G10.
- [13] Melvin L Selzer and Amiram Vinokur. 1974. Life events, subjective stress, and traffic accidents. *American Journal of Psychiatry* 131, 8 (1974), 903–906.
- [14] Ye Sun and Xiong Bill Yu. 2014. An innovative noninvasive driver assistance system for vital signal monitoring. *IEEE journal of biomedical and health informatics* 18, 6 (2014), 1932–1939.
- [15] Zephyr Performance Systems. [n. d.]. Zephyr BioModule Device. ([n. d.]). <https://www.zephyranywhere.com/benefits/physiological-biomechanical>.
- [16] Adrian H Taylor and Lisa Dorn. 2006. Stress, fatigue, health, and risk of road traffic accidents among professional drivers: the contribution of physical inactivity. *Annu. Rev. Public Health* 27 (2006), 371–391.
- [17] José Vicente, Pablo Laguna, Ariadna Bartra, and Raquel Bailón. 2016. Drowsiness detection using heart rate variability. *Medical & Biological Engineering & Computing* 54, 6 (01 Jun 2016), 927–937. <https://doi.org/10.1007/s11517-015-1448-7>
- [18] Qi Zhang, Guo-qing Xu, Ming Wang, Yimin Zhou, and Wei Feng. [n. d.]. Webcam based non-contact real-time monitoring for the physiological parameters of drivers. In *Cyber Technology in Automation, Control, and Intelligent Systems (CYBER), 2014 IEEE 4th Annual International Conference on*.